



SHORT COMMUNICATION

A novel mutation in *COL1A2* leads to osteogenesis imperfecta/Ehlers-Danlos overlap syndrome with brachydactyly

Thunyaporn Budsamongkol ^a, Narin Intarak ^b,
 Thanakorn Theerapanon ^c, Somchai Yodsanga ^d,
 Thantrira Porntaveetus ^{a,b,*}, Vorasuk Shotelersuk ^{e,f}

^a Geriatric Dentistry and Special Patients Care International Program, Faculty of Dentistry, Chulalongkorn University, Bangkok, 10330, Thailand

^b Genomics and Precision Dentistry Research Unit, Department of Physiology, Faculty of Dentistry, Chulalongkorn University, Bangkok, 10330, Thailand

^c Center of Excellence for Regenerative Dentistry, Faculty of Dentistry, Chulalongkorn University, Bangkok, 10330, Thailand

^d Biomaterial Testing Center, Faculty of Dentistry, Chulalongkorn University, Bangkok, 10330, Thailand

^e Center of Excellence for Medical Genomics, Department of Pediatrics, Faculty of Medicine, Chulalongkorn University, Bangkok, 10330, Thailand

^f Excellence Center for Medical Genetics, King Chulalongkorn Memorial Hospital, The Thai Red Cross Society, Bangkok, 10330, Thailand

Received 12 November 2018; accepted 13 March 2019

Available online 16 March 2019

KEYWORDS

Bone-like dentin;
 Collagen defect;
 Dentinogenesis
 imperfecta;
 Joint laxity;
 Skeletal fragility;
 Skin hypermobility

Abstract Osteogenesis imperfecta (OI) is mainly characterized by bone fragility and Ehlers-Danlos syndrome (EDS) by connective tissue defects. Mutations in *COL1A1* or *COL1A2* can lead to both syndromes. OI/EDS overlap syndrome is mostly caused by helical mutations near the amino-proteinase cleavage site of type I procollagen. In this study, we identified a Thai patient having OI type III, EDS, brachydactyly, and dentinogenesis imperfecta. His dentition showed delayed eruption, early exfoliation, and severe malocclusion. For the first time, ultrastructural analysis of the tooth affected with OI/EDS showed that the tooth had enamel inversion, bone-like dentin, loss of dentinal tubules, and reduction in hardness and elasticity, suggesting severe developmental disturbance. These severe dental defects have never been reported in OI or EDS. Exome sequencing identified a novel *de novo* heterozygous glycine substitution, c.3296G > A, p.Gly1099Glu, in exon 49 of *COL1A2*. Three patients with mutations in the exon

* Corresponding author. Genomics and Precision Dentistry Research Unit, Department of Physiology, Faculty of Dentistry, Chulalongkorn University, Bangkok, 10330, Thailand. Fax: +662 218 8691.

E-mail address: thantrira.p@chula.ac.th (T. Porntaveetus).

Peer review under responsibility of Chongqing Medical University.

49 of *COL1A2* were previously reported to have OI with brachydactyly and intracranial hemorrhage. Notably, two of these three patients did not show hyperextensible joints and hypermobile skin, while our patient at the age of 5 years had not developed intracranial hemorrhage. Here, we demonstrate that the novel glycine substitution in the carboxyl region of $\alpha 2(I)$ collagen triple helix leads to OI/EDS with brachydactyly and severe tooth defects, expanding the genotypic and phenotypic spectra of OI/EDS overlap syndrome.

Copyright © 2019, Chongqing Medical University. Production and hosting by Elsevier B.V. This is an open access article under the CC BY-NC-ND license (<http://creativecommons.org/licenses/by-nc-nd/4.0/>).

Introduction

Osteogenesis imperfecta (OI) is a group of inherited connective tissue disorders mainly characterized by bone fragility, growth deficiency, and blue sclera. Mutations in the *COL1A1* or *COL1A2* genes that encode pro- $\alpha 1$ and pro- $\alpha 2(I)$ chains of type I procollagen have been found in the majority of patients with OI. Of those, the missense mutations especially glycine substitutions in the triple-helical domain of the pro- $\alpha 1(I)$ and pro- $\alpha 2(I)$ chains are the most common.¹

Ehlers-Danlos syndrome (EDS) is a group of genetic connective tissue disorders characterized by hypermobile joints, loose skin, and fragile tissues. Heterozygous mutations in *COL1A1* or *COL1A2* lead to EDS, arthrochalasia type 1 (VIA, OMIM #130060) and arthrochalasia type 2 (VIIB, OMIM #617821) when they affect exon 6 of either gene and prohibit cleavage of the amino-propeptide of procollagen type I.^{2,3} Homozygous or compound heterozygous *COL1A2* mutations are associated with the cardiac-valvular type of EDS (OMIM # 225320).^{4,5}

The combination of OI and EDS is very rare. Most mutations causing OI/EDS are observed in the amino terminal part of type I collagen genes. They have been shown to interfere the N-cleavage sites and interhelical cross-linking of collagen chains.^{6,7}

Brachydactyly is a form of bone dysostosis referring to the shortening of hands and/or feet, affecting the phalanges and/or metacarpal/metatarsal bones.⁸ It is present as an isolated feature or as a part of syndromes, but not usually found in OI. For the first time, a study of Montreal cohort proposed that OI type III with brachydactyly and intracranial hemorrhage is associated with mutations in the exon 49 of *COL1A2*.⁹ To date, their hypothesis has not been confirmed.

Our study demonstrates a patient having a combination of OI type III, EDS, brachydactyly, diverse craniofacial anomalies, and abnormal dentin which has never been reported in OI or EDS. The novel *de novo* glycine substitution affecting the most carboxy-terminal part of the collagen type I $\alpha 2$ chain has been identified. These reveal the new insight and expand genotypic and phenotypic spectra of OI/EDS overlap syndrome.

Material and methods

A Thai boy and his parents were recruited. This study was conducted in full accordance with the World Medical

Association Declaration of Helsinki (version 2008) and the additional requirements. It was exempted from review by the Institutional Review Board (IRB631/60), Faculty of Medicine, Chulalongkorn University. The research was performed with the understanding and written consent of each participant.

Mutation analysis

The genomic DNA extracted from peripheral blood leukocytes was prepared according to a previous publication.¹⁰ Filtering criteria were demonstrate in [Supplementary data S1](#).

Analysis of tooth ultrastructures

The exfoliated lower right central incisor of the proband was investigated as previously described.¹¹ Briefly, tooth color was measured as L*a*b* scale by ShadeEye-NCC® (Shofu Inc., Japan). Cross section and mineral density of the teeth were analyzed by micro-computerized tomography (uCT35, Scanco Medical, Switzerland). Nanohardness and elastic modulus were measured by the Ultra Micro-Indentation System (UMIS II, CSIRO, Australia) at 1–200 mN for 30 spots. Scanning electron microscope (SEM; Quanta 250, FEI, Hillsboro, OR, USA) was used to examine the ultrastructures of enamel and dentin. The specimens were decalcified, sectioned, and stained with hematoxylin and eosin and Masson's trichrome.

Results

Clinical and radiographic manifestations

The proband was a 4-year-old boy ([Fig. 1a](#)). His parents were non-consanguineous and healthy. He was delivered at 35 weeks of gestation by cesarean section due to premature rupture of membranes. His birth weight was 1840 g (<-3 SD). Apgar scores were 9, 10, 10. He was born with body deformity, tachypnea, bowed legs, fracture of the right femoral shaft, and tongue tie ([Fig. 1b](#)). Clinical and radiographic examinations at age 12 days showed a fracture of his right femur, bowing of extremities, bell shaped chest, plagiocephaly, prominent forehead, blue sclerae, and low-set ears. The diagnosis of OI type III was given. Cyclical intravenous pamidronate therapy was initiated and continued every 2 months. The radiographs at age 3 months showed closed



Figure 1 Physical characteristics of the proband. **a** Photographs taken at 4 years of age showed short stature, prominent forehead, low-set ears, blue sclerae, and bowing of extremities. **b** Whole body radiograph at age 11 days showed body deformity, curved long bones, and fracture of right femoral shaft immobilized with a cast. **c** Radiographs at age 3 months exhibited closed fracture of right femur, bowing of left femur and bilateral tibiae, malformed humeri, and multiple fractures of right ribs. **d, e** The cranial vault was misshaped tilting upward to the right. **f-i** radiographs at age 3 years showed curvatures of radii, femora, tibiae, thin diaphyses of long bones especially the fibulae, small thorax, mild levoscoliosis of thoracolumbar spines, cortical thinning of bilateral ribs and codfish vertebrae, and mild deformity of right posterior 5th – 8th ribs. **j-p** The patient at 3.5 years had curved extremities, flexible joint, flat feet, stretchy skin, flexible joint, short fingers and toes. **q, r** The phalangeal bones were short especially the distal phalanges.

fracture of his right femur, bowing of his left femur and bilateral tibiae, malformed humeri, and multiple fractures of his right ribs (Fig. 1c). He developed tachypnea with rapid shallow breathing and subcostal retraction, possibly due to

ribs anomaly. He had plagiocephaly and soft cranial vault which was tilted upward to the right (Fig. 1d, e).

No bone fractures had been observed during pamidronate treatment, except when the proband fell from his

toddler tricycle at the age of 2 years 9 months causing fractures of his right humerus. At 3 years of age, curvatures of radii, femora, and tibiae, thin diaphyses of long bones especially the fibulae, angulated right humerus, small thorax, mild levoscoliosis of thoracolumbar spines, cortical thinning of bilateral ribs, codfish vertebrae, and mild deformity of right posterior 5th - 8th ribs were observed (Fig. 1f–i). Other anomalies apart from OI were detected including highly elastic and fragile skin, generalized joint hypermobility, broad hands, short fingers and toes, large thumbs, leg length discrepancy (right 29 cm; left 34 cm), flat feet, and genu recurvatum with abduction of the feet (Fig. 1j–p). Passive dorsiflexion of his index finger was beyond 90° touching the back of his hand. Radiologically, short phalangeal bones and thin diaphysis especially the distal phalanges were present, suggesting brachydactyly (Fig. 1q, r). His nails were unremarkable. The parents and other family members did not have a history of bone fractures, digital anomalies, and joint hypermobility. The Z-score of lumbar spine BMD was -4.38 , -9 , -3.6 at the age of 12 days, 7 months, and 42 months respectively, indicating a severe osteoporosis in the proband. At the age of 5 years 8 months, his serum levels of osteocalcin was 32.91 ng/mL (42.1 – 128.2); total procollagen type1 amino propeptide (P1 NP) was 165.40 ng/mL (111.5 – 768.4)¹²; B-CrossLaps was 0.68 ng/mL (0.92 – 1.42)¹³; and total vitamin D (25OH) was 40.2 ng/mL (20 – 100). The level of P1 NP, a bone formation marker, was within the normal range while the level of B-CrossLaps, a bone resorption marker was low. These markers suggest that bone formation in the proband was at a normal rate. However, the synthesized collagen had aberrant structure due to the mutation. Therefore, even with pamidronate administration to slow the rate of bone resorption, the proband's BMD was still lower than the normal range. Physical parameters of the patient were summarized in [Supplementary Table S2](#).

Craniofacial characteristics

The proband's cranial vault at age 3 years was misshapen. He had large anterior (W*L; 10×11 cm) and posterior fontanelles (3×3 cm), separated sagittal and coronal sutures, wormian bones, class III malocclusion, underdeveloped maxilla, and anterior and lateral openbite (Fig. 2a–c). His bone age and tooth development were delayed. Tooth eruption started at 16 months and was completed at 3.4 years of age. All of his teeth had dentinogenesis imperfecta and were rapidly deteriorated after eruption (Fig. 2d–f). Dental radiographs revealed very thin enamel and dentin, large pulp cavities, and curved roots (Fig. 2g–l). At age 2.5 years, his lower right central incisor was spontaneously exfoliated.

Tooth ultrastructure

The exfoliated lower central incisor was subjected for investigations. The color of proband's tooth (L value, 70.6 ; a value, 5.7 ; b value, 16.0) was darker, redder, and yellower than the control (L, 77.1 , a, -1.3 , b, 10.5). The tooth was severely malformed. It had several deep grooves and pits on the enamel and voids in the dentin. The dentin was

opalescent and the roots were short. The proband's dentin contained scattering layers of amorphous calcified sheathes. In contrast, the regular orientation of dentinal tubules was observed in the control dentin and united calcified structure was found in the dentin of another OI patient (Fig. 3a–f). SEM of the proband's tooth revealed an amorphous structure of the dentin containing unorganized calcified masses and loss of typical dentinal tubules (Fig. 3i, j). Its dentinoenamel junction contained gap and mineralized mass and did not show the usual scallop pattern of the junction, suggesting the anomalous enamel-dentin connection (Fig. 3o, p). The enamel rods of the proband's tooth were rounder, shorter, and contained much less collagen fibrils, compared with the controls (Fig. 3q, r). Histologically, the pattern of haversian system similar to bone was observed in the proband's dentin while the dentinal tubules were found in the control (Fig. 3k–n). The hardness and elasticity of proband's enamel and dentin were significantly lower than those of the controls (Fig. 3s and [Supplementary Table S3](#)). Micro-computerized tomography identified that the mineral densities of the proband's enamel and dentin were 2098.24 and 1232.74 mgHA/cm³ respectively, which were comparable to the control enamel (2070.92 mgHA/cm³) and dentin (1205.87 mgHA/cm³). Therefore, the abnormal structure or quality of collagen is more likely than the decreased level of calcification to cause the proband's tooth defects.

Genetic investigation

Chromosomal study of the proband revealed a normal male karyotype. Mutation analysis was performed by whole-exome sequencing (WES). Total yield of 5230 Mbp was achieved. The capture efficiency was 93.8% more than 10X. The mean read depth of target regions was 66.1X. Sanger sequencing of the candidate variants was performed in the proband and his parents. We identified that the proband harbored a novel *de novo* missense mutation, c.3296G > A, p.Gly1099Glu, in exon 49 of the *COL1A2* gene (NM_000089.3), resulting in a glycine to glutamate change in the collagen triple helix repeat of *COL1A2* (Fig. 4a, b). This position was highly conserved among several species (human, cattle, rabbit, mouse, frog, and zebrafish) (Fig. 4c). The p.Gly1099Glu was predicted to be probably damaging (PolyPhen2: 1.0), damaging (SIFT: 0.001), possibly pathogenic (M-CAP: 0.881), and pathogenic (ACMG).¹⁴ Visualization of *COL1A2* showed that the mutant residue was bigger in size, more hydrophobic, and less flexibility than the wild type. These was expected to cause a negative charge to the mutant protein, incorrect back-bone conformation, and disturb protein structure (Fig. 4e–g).¹⁵ Neither his parents harbored the p.Gly1099Glu mutation in *COL1A2*.

Discussion

Our study demonstrates the novel mutation in the carboxyl-terminus of *COL1A2* that leads to type III OI/EDS overlap syndrome with brachydactyly and diverse oro/dento/craniofacial anomalies.

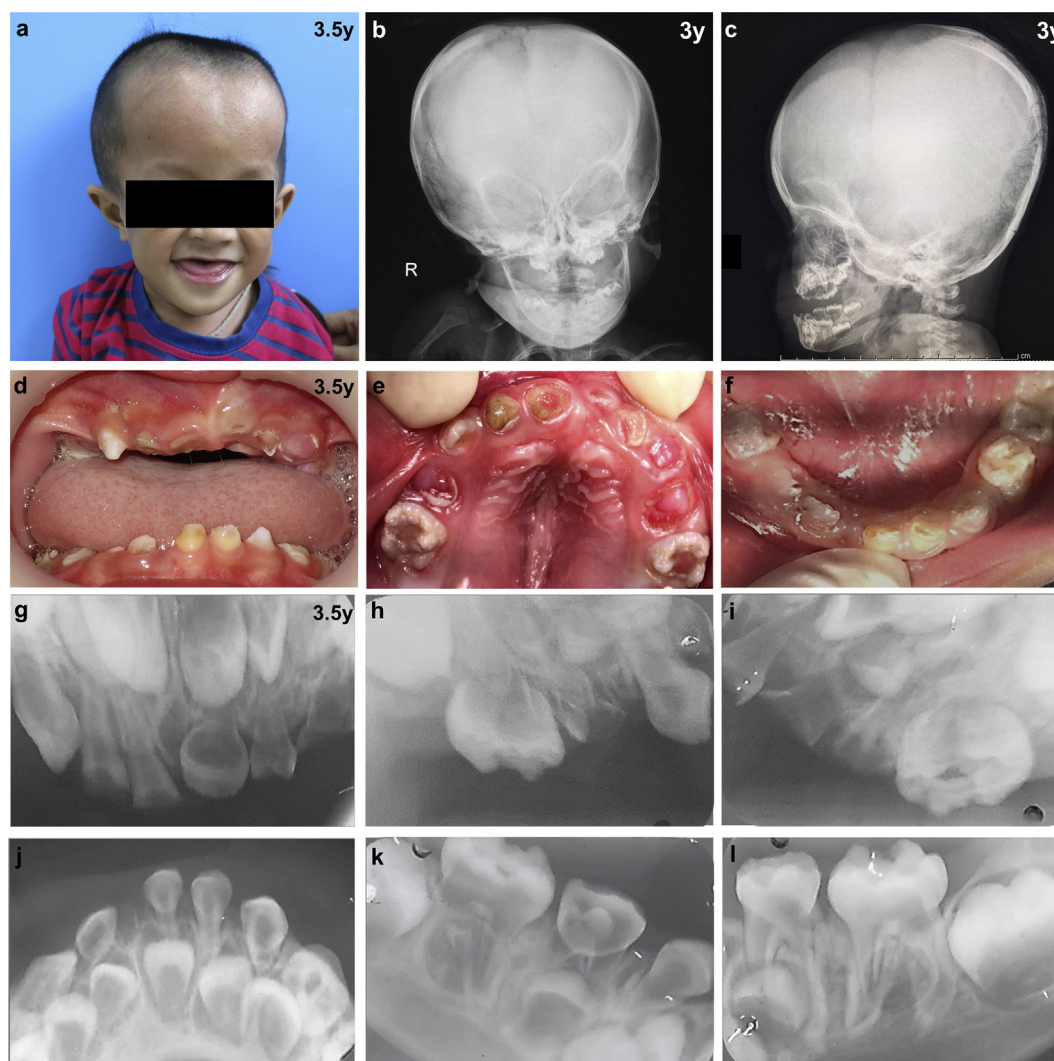


Figure 2 Craniofacial manifestations of the proband. **a** Frontal photograph at age 3.5 years of age showed head asymmetry, soft forehead, and blue sclerae. **b, c** Cranial radiographs revealed opened anterior fontanelle, separated sagittal and coronal sutures, wormian bones, underdeveloped maxilla, and openbite. **d-f** His primary teeth had dentinogenesis imperfecta, severe deterioration exposing dentin and pulp, and malocclusion. The lower right central incisor was early exfoliated. **g-l** Dental radiographs exhibited large pulp, thin enamel with reduced radiopacity, curved roots, and multiple retained roots.

OI is a heritable connective tissue disorder with wide phenotypic and genotypic spectra. It comprises up to eighteen types which are associated with twenty different genes.¹ Almost 90% of OI individuals have mutations in *COL1A1* or *COL1A2* gene. Eighty percent of those are helical glycine substitution.¹⁶ More than 350 substitutions of glycine residues have been observed across *COL1A2* gene (<http://www.le.ac.uk/ge/collagen/>). While the mutations in *COL1A1* or *COL1A2* causing OI have been observed randomly across the genes, the mutations causing EDS are more specific. Homozygous or compound heterozygous mutations in *COL1A2* leading to nonsense-mediated decay or complete deficiency of $\alpha 2(I)$ collagen chain have been associated with cardiac-valvular type of EDS.^{17,18} The heterozygous *COL1A2* mutations leading to skipping of exon 6 near the cleavage site of procollagen type I-N-proteinase have been found in arthrochalasia type of EDS.¹⁹ The pathogenic variants causing hypermobile EDS remain

largely unknown but are believed to be associated with *COLA1* or *COL1A2* mutations.²⁰ There have been a few reports in OI/EDS showing that the heterozygous mutations located adjacent to the cleavage site of procollagen N-proteinase in the amino terminus of either $\alpha 1$ or $\alpha 2(I)$ -collagen helix are responsible for most OI/EDS cases.^{7,18,21–23} These mutations interfere the N-propeptide cleavage, resulting in the formation of small and weak collagen fibrils.^{6,24} In this study, we have identified the mutation in exon 49 of *COL1A2* associated with OI/EDS phenotype. This proposes that glycine substitution in the carboxyl terminus of $\alpha 2(I)$ -collagen could also cause OI/EDS.

Genotype-phenotype correlation gives clues to general developmental biology and is important for genetic counseling.^{25,26} It has been shown that the mutations affecting glycine residues in the Gly-X-Y triplet domain of the type I collagen triple helix, compared with haploinsufficiency

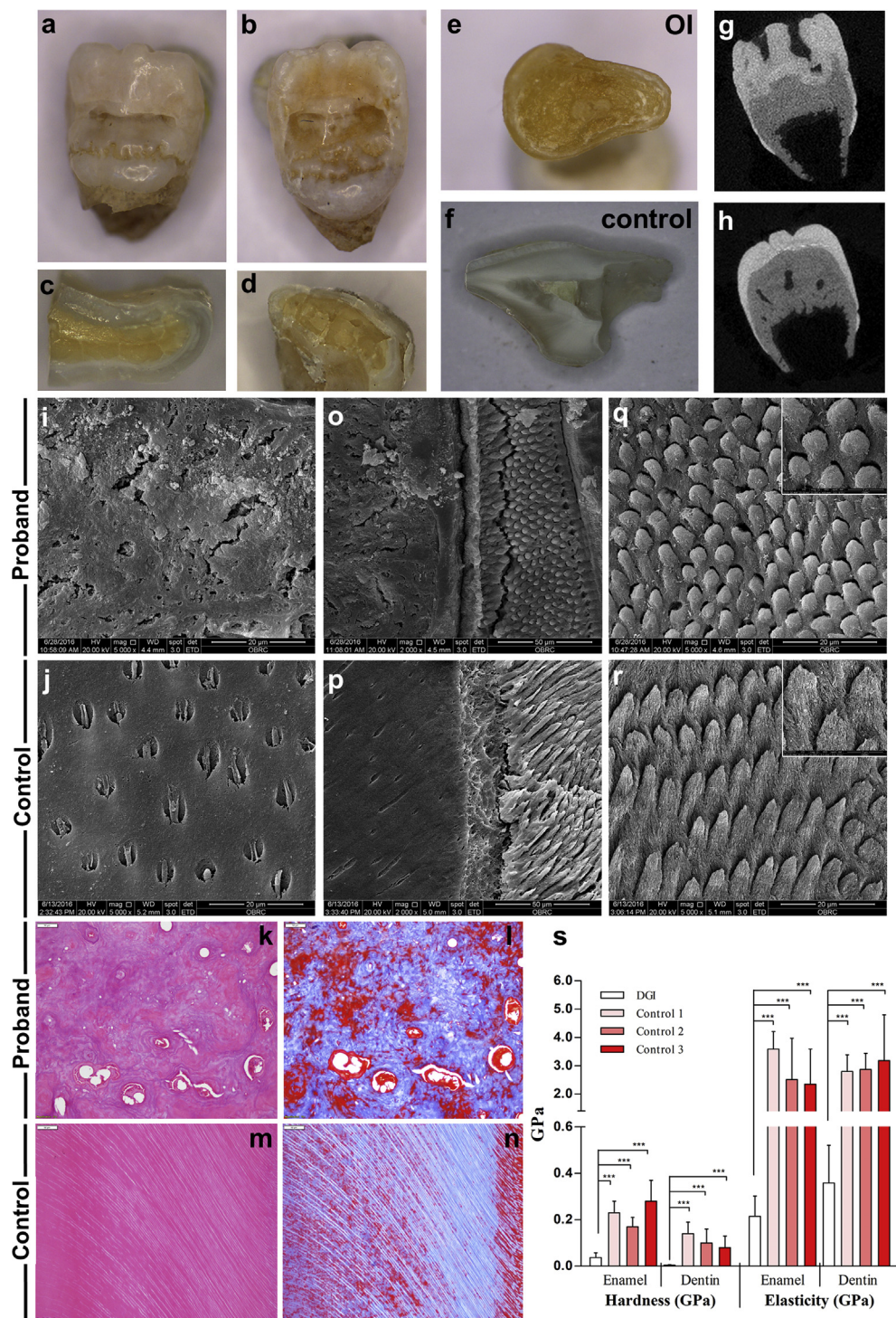


Figure 3 Dental ultrastructures. **a-d** The proband's lower right central incisor exfoliated at 2.5 years of age showed extensive defects including very short root, several enamel pits and grooves, opalescent dentin containing multiple scattered layers. **e** The dentin of primary tooth affected with dentinogenesis imperfecta from another OI patient exhibited ununited opalescent structure. **f** The primary incisor from healthy individual showed regular arrangement of dentinal tubules. **g, h** Micro computerized tomography of the proband's incisor showed inversion of enamel and holes in the dentin. **i-r** The proband's tooth showed amorphous dentin, anomalous dentinoenamel junction, and short enamel rods while the control showed regular arrangement of dentinal tubules, scallop dentinoenamel junction, and prism-shaped enamel rods. **k-n** Histological sections of proband's tooth showed harversian system. **s** The proband's enamel and dentin showed significant reduction in hardness and elasticity compared to the controls.

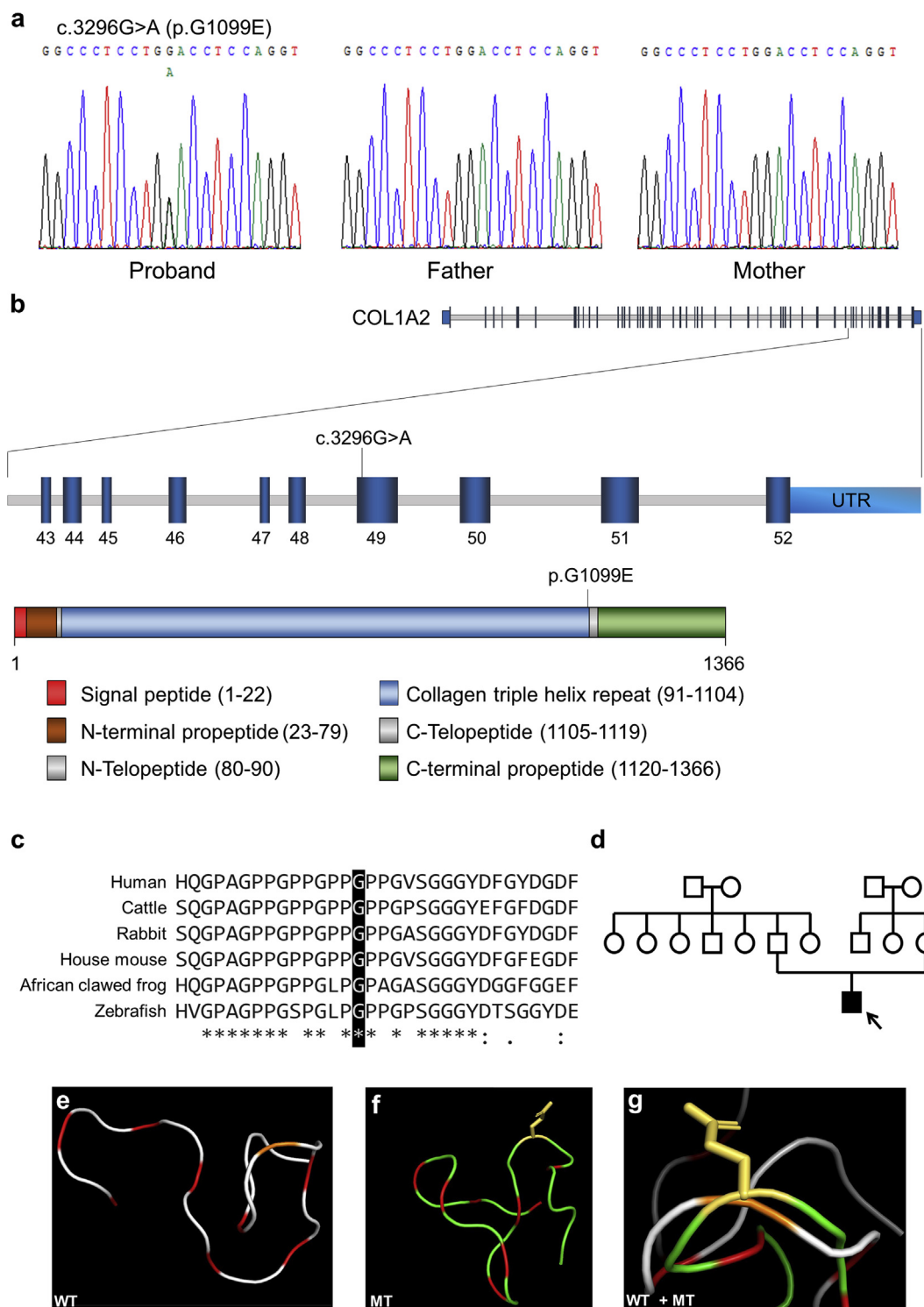


Figure 4 Genetic investigations. **a** Sequence chromatograms demonstrated the presence of the novel *de novo* heterozygous missense mutation, c.3296G > A, p.G1099E, in exon 49 of the COL1A2 gene (NM_000089.3) in the proband. The parents did not possess the mutation. **b** Schematic diagrams indicated the mutation above the exon 49 of COL1A2 and collagen triple helix repeat domain of the COL1A2 proteins (NP_000080.2). **c** Sequence alignment of partial amino acid sequence of COL1A2 showed the conservation of the glycine-1099 across species indicated by a black box. **d** Pedigree of the family. The arrow marked the proband. The blackened symbols represented affected individual. **e-g** Diagram showed the region of COL1A2 affected by the mutation. Differences in size and structure were shown between wild-type p.Gly1099 (orange) and mutant p.Glu1099 (yellow). Glycine position was demonstrated in red. WT, wild type; MT, mutant.

mutations, are responsible for more severe phenotypes including extensive skeletal abnormalities, low bone mineral density, short stature, dentinogenesis imperfecta, and scoliosis.^{27,28} However, there was no definite genotype–phenotype correlation among the helical glycine mutations.

The patients with severe forms of OI usually present with malocclusion.^{29,30} Dentinogenesis imperfecta is mostly found when glycine substitution is positioned carboxyl terminal to p.Gly211.³¹ Correspondingly, the proband had severe malocclusion, mandibular prognathism, underdeveloped maxilla, and dentinogenesis imperfecta. In addition, the significant reduction in hardness and elasticity and the unique bone-like dentin were observed in the proband's tooth. These have never been reported in OI or EDS.

The shortness of long bones is a typical characteristic of OI, but short hands and feet are uncommon. We found that our patient had short phalangeal bones without a history of finger fractures. A previous study by Faeih et al, 2009 reported three OI patients out of their 153 OI cohort. They proposed for the first time that the glycine substitutions, p.Gly1090Asp, p.Gly1096Ala, and p.Gly1099Arg, in exon 49 of *COL1A2* could lead to OI type III, brachydactyly, and intracranial hemorrhage.⁹ To our knowledge, no other reports apart from the aforementioned study have demonstrated the relationship between the *COL1A2* glycine substitution and brachydactyly. The p.Gly1099Glu mutation found in the proband in this study is located at the same glycine residue as the reported p.G1099Arg,⁹ but results in different amino acid change. Many lines of evidences suggest that the p.Gly1099Glu is pathogenic. Firstly, it is absent in his healthy parents, HGMD, ExAC, OI variant databases, and our in-house database. Secondly, *in silico* analyses predict it as damaging (SIFT: 0.001), probably damaging (PolyPhen2: 1.0), and possibly pathogenic (MCAP: 0.881). The glycine-1099 is highly conserved among species. Thirdly, the mutation is expected to change the Gly-X-Y repeating pattern in the collagen triple helix. This could disturb local hydrogen bonding and destabilize the triple helix integrity.³² Notably, none of the other 34 patients with OI in our Thai cohort have brachydactyly. Our findings strengthen the statement that the substitutions at the glycine-1099 of *COL1A2* are associated with brachydactyly in OI type III.

Faeih et al, 2009 also proposed that the *COL1A2* mutations in exon 49 were associated with intracranial hemorrhage.⁹ However, the p.Gly1099Arg patient did not have spontaneous intracranial bleeding but developed epidural hematoma after falling off a wheelchair at the age of 6.5 years.⁹ At the last follow-up, the proband at the age of 5 years 8 months had not had any signs of intracranial bleeding. Whether the glycine-1099 mutations increase the risk of intracranial bleeding therefore requires further studies.

The triple helix is the fundamental structure of collagens which are the most abundant protein in the human body. Glycine, the smallest amino acid, is found in every third residue of the triple helix. The substitutions of glycine with another amino acid which is bigger, charged, and has extended side chain are expected to impede helix formation and collagen processing causing tissue deformities. These could lead to a mixture of collagen problems involving bone

fragility, loose joints, stretchy skin, intracranial hemorrhage, abnormal dentin, cardiac-valvular problems, pneumothorax, and hip dislocation.

In conclusion, we report the novel mutation in the carboxyl terminus of *COL1A2* in the patient who has OI/EDS, brachydactyly, and severe dental anomalies, but not intracranial hemorrhage. These expand phenotypic and genotypic spectra related to OI/EDS overlap syndrome. Our study also substantiates the previously hypothesized genotype–phenotype correlation stating that glycine substitutions in the most carboxy-terminal part of the collagen type I alpha 2 chain are explicitly associated with brachydactyly in OI patients.

Author's contributions

TB, TP, VS contributed to conception, data analysis, drafting, and critical revision of the manuscript; TT, NI, SY contributed to data acquisition and critical revision of the manuscript. All authors gave final approval and agree to be accountable for all aspects of the work.

Conflict of interest

All authors declare that they have no conflict of interest.

Acknowledgements

This study was supported by the 90th Anniversary of Chulalongkorn University, Rachadapisek Sompote Fund; Faculty of Dentistry (DFR62003), Chulalongkorn University; Chulalongkorn Academic Advancement Into Its 2nd Century Project; Newton Fund; Thailand Research Fund (RSA6280001, DPG6180001), Thailand. NI is supported by Ratchadapisek Somphot Fund for Postdoctoral Fellowship, Chulalongkorn University, Thailand. We thank Trakarn Sookthonglarng and Yuttupong Kunchanapruek for blood collection, and Lawan Boonprakong for SEM.

Appendix A. Supplementary data

Supplementary data to this article can be found online at <https://doi.org/10.1016/j.jgendis.2019.03.001>.

References

1. Marini JC, Forlino A, Bachinger HP, et al. Osteogenesis imperfecta. *Nat Rev Dis Primers*. 2017;3:17052.
2. D'Hondt S, Van Damme T, Malfait F. Vascular phenotypes in nonvascular subtypes of the Ehlers-Danlos syndrome: a systematic review. *Genet Med*. 2018;20:562–573.
3. Byers PH, Duvic M, Atkinson M, et al. Ehlers-Danlos syndrome type VIIA and VIIB result from splice-junction mutations or genomic deletions that involve exon 6 in the *COL1A1* and *COL1A2* genes of type I collagen. *Am J Med Genet*. 1997;72:94–105.
4. Schwarze U, Hata R-I, McKusick VA, et al. Rare autosomal recessive cardiac valvular form of Ehlers-Danlos syndrome results from mutations in the *COL1A2* gene that activate the

- nonsense-mediated RNA decay pathway. *Am J Hum Genet.* 2004;74:917–930.
5. Malfait F, Symoens S, Coucke P, Nunes L, De Almeida S, De Paepe A. Total absence of the alpha2(I) chain of collagen type I causes a rare form of Ehlers-Danlos syndrome with hypermobility and propensity to cardiac valvular problems. *J Med Genet.* 2006;43:e36.
 6. Makareeva E, Cabral WA, Marini JC, Leikin S. Molecular mechanism of alpha 1(I)-osteogenesis imperfecta/Ehlers-Danlos syndrome: unfolding of an N-anchor domain at the N-terminal end of the type I collagen triple helix. *J Biol Chem.* 2006;281:6463–6470.
 7. Malfait F, Symoens S, Goemans N, et al. Helical mutations in type I collagen that affect the processing of the amino-propeptide result in an Osteogenesis Imperfecta/Ehlers-Danlos Syndrome overlap syndrome. *Orphanet J Rare Dis.* 2013;8:78.
 8. Jagadeesh KA, Wenger AM, Berger MJ, et al. M-CAP eliminates a majority of variants of uncertain significance in clinical exomes at high sensitivity. *Nat Genet.* 2016;48:1581–1586.
 9. Faqeih E, Roughley P, Glorieux FH, Rauch F. Osteogenesis imperfecta type III with intracranial hemorrhage and brachydactyly associated with mutations in exon 49 of COL1A2. *Am J Med Genet A.* 2009;149a:461–465.
 10. Porntaveetus T, Srichomthong C, Ohazama A, Suphapeetiporn K, Shotelersuk V. A novel GJA1 mutation in oculodentodigital dysplasia with extensive loss of enamel. *Oral Dis.* 2017;23:795–800.
 11. Porntaveetus T, Osathanon T, Nowwarote N, et al. Dental properties, ultrastructure, and pulp cells associated with a novel DSPP mutation. *Oral Dis.* 2018;24:619–627.
 12. Bayer M. Reference values of osteocalcin and procollagen type I N-propeptide plasma levels in a healthy Central European population aged 0-18 years. *Osteoporos Int.* 2014;25:729–736.
 13. Herrmann D, Intemann T, Lauria F, et al. Reference values of bone stiffness index and C-terminal telopeptide in healthy European children. *Int J Obes.* 2014;38:S76.
 14. Richards S, Aziz N, Bale S, et al. Standards and guidelines for the interpretation of sequence variants: a joint consensus recommendation of the American college of medical genetics and genomics and the association for molecular pathology. *Genet Med.* 2015;17:405–424.
 15. Schrödinger LLC. *The AxPyMOL Molecular Graphics Plugin for Microsoft PowerPoint, Version 1.0.* 2010.
 16. Lindahl K, Åström E, Rubin C-J, et al. Genetic epidemiology, prevalence, and genotype–phenotype correlations in the Swedish population with osteogenesis imperfecta. *Eur J Hum Genet.* 2015;23:1042–1050.
 17. Nicholls AC, Osse G, Schloon HG, et al. The clinical features of homozygous alpha 2(I) collagen deficient osteogenesis imperfecta. *J Med Genet.* 1984;21:257–262.
 18. Nicholls AC, Valler D, Wallis S, Pope FM. Homozygosity for a splice site mutation of the COL1A2 gene yields a non-functional pro(alpha)2(I) chain and an EDS/OI clinical phenotype. *J Med Genet.* 2001;38:132–136.
 19. Klaassens M, Reinstein E, Hilhorst-Hofstee Y, et al. Ehlers-Danlos arthrochalasia type (VIIA-B)-expanding the phenotype: from prenatal life through adulthood. *Clin Genet.* 2012;82:121–130.
 20. Malfait F, Clair F, Peter B, et al. The 2017 international classification of the Ehlers–Danlos syndromes. *Am J Med Genet C.* 2017;175:8–26.
 21. Feshchenko S, Brinckmann J, Lehmann HW, Koch HG, Muller PK, Kugler S. Identification of a new heterozygous point mutation in the COL1A2 gene leading to skipping of exon 9 in a patient with joint laxity, hyperextensibility of skin and blue sclerae. Mutations in brief no. 166. Online. *Hum Mutat.* 1998;12:138.
 22. Nicholls AC, Oliver J, Renouf DV, Heath DA, Pope FM. The molecular defect in a family with mild atypical osteogenesis imperfecta and extreme joint hypermobility: exon skipping caused by an 11-bp deletion from an intron in one COL1A2 allele. *Hum Genet.* 1992;88:627–633.
 23. Raff ML, Craigen WJ, Smith LT, Keene DR, Byers PH. Partial COL1A2 gene duplication produces features of osteogenesis imperfecta and Ehlers-Danlos syndrome type VII. *Hum Genet.* 2000;106:19–28.
 24. Cabral WA, Makareeva E, Colige A, et al. Mutations near amino end of alpha1(I) collagen cause combined osteogenesis imperfecta/Ehlers-Danlos syndrome by interference with N-propeptide processing. *J Biol Chem.* 2005;280:19259–19269.
 25. Sangsin A, Kuptanon C, Srichomthong C, Pongpanich M, Suphapeetiporn K, Shotelersuk V. Two novel compound heterozygous BMP1 mutations in a patient with osteogenesis imperfecta: a case report. *BMC Med Genet.* 2017;18:25.
 26. Tongkobpetch S, Limpaphayom N, Sangsin A, Porntaveetus T, Suphapeetiporn K, Shotelersuk V. A novel de novo COL1A1 mutation in a Thai boy with osteogenesis imperfecta born to consanguineous parents. *Genet Mol Biol.* 2017;40:763–767.
 27. Rauch F, Lalic L, Roughley P, Glorieux FH. Relationship between genotype and skeletal phenotype in children and adolescents with osteogenesis imperfecta. *J Bone Miner Res.* 2010;25:1367–1374.
 28. Lin H-Y, Chuang C-K, Su Y-N, et al. Genotype and phenotype analysis of Taiwanese patients with osteogenesis imperfecta. *Orphanet J Rare Dis.* 2015;10:152.
 29. Rizkallah J, Schwartz S, Rauch F, et al. Evaluation of the severity of malocclusions in children affected by osteogenesis imperfecta with the peer assessment rating and discrepancy indexes. *Am J Orthod Dentofacial Orthop.* 2013;143:336–341.
 30. Chang PC, Lin SY, Hsu KH. The craniofacial characteristics of osteogenesis imperfecta patients. *Eur J Orthod.* 2007;29:232–237.
 31. Andersson K, Dahllöf G, Lindahl K, et al. Mutations in COL1A1 and COL1A2 and dental aberrations in children and adolescents with osteogenesis imperfecta – a retrospective cohort study. *PLoS One.* 2017;12, e0176466.
 32. Folkestad L, Hald JD, Canudas-Romo V, et al. Mortality and causes of death in patients with osteogenesis imperfecta: a register-based nationwide cohort study. *J Bone Miner Res.* 2016;31:2159–2166.